Provably Good Moving Least Squares

RAVIKRISHNA KOLLURI

University of California, Berkeley

Abstract. We analyze a *moving least squares* (MLS) interpolation scheme for reconstructing a surface from point cloud data. The input is a sufficiently dense set of sample points that lie near a closed surface F with approximate surface normals. The output is a reconstructed surface passing near the sample points. For each sample point s in the input, we define a linear *point function* that represents the local shape of the surface near s. These point functions are combined by a weighted average, yielding a three-dimensional function I. The reconstructed surface is implicitly defined as the zero set of I.

We prove that the function I is a good approximation to the signed distance function of the sampled surface F and that the reconstructed surface is geometrically close to and isotopic to F. Our sampling requirements are derived from the *local feature size* function used in Delaunay-based surface reconstruction algorithms. Our analysis can handle noisy data provided the amount of noise in the input dataset is small compared to the feature size of F.

Categories and Subject Descriptors: I.3.5 [**Computer Graphics**]: Computational Geometry and Object Modeling—*Curve, surface, solid, and object representations*

General Terms: Theory, Algorithms

Additional Key Words and Phrases: Reconstruction, interpolation, implicit surfaces

ACM Reference Format:

Kolluri, R. 2008. Provably good moving least squares. ACM Trans. Algor. 4, 2, Article 18 (May 2008), 25 pages. DOI = 10.1145/1361192.1361195 http://doi.acm.org/10.1145/1361192.1361195

1. *Introduction*

Surface reconstruction algorithms are used to define surfaces from point cloud data generated from real-world objects by laser range scanners, computer vision techniques, or other methods. In this article, we analyze a moving least-squares (MLS) scheme for reconstructing surfaces from point cloud data. The input to our method is a set of sample points S close to the surface F of a smooth, closed, orientable 3D-object. For each sample point in $s \in S$, a normal vector that approximates the

This article is an extended version of the paper presented at SODA'05.

This work was supported in part by the National Science Foundation under awards CCR-0204377 and CCF-0430065 and in part by a gift from the Okawa Foundation.

Author's address: University of California, Berkeley; email: rkolluri@gmail.com.

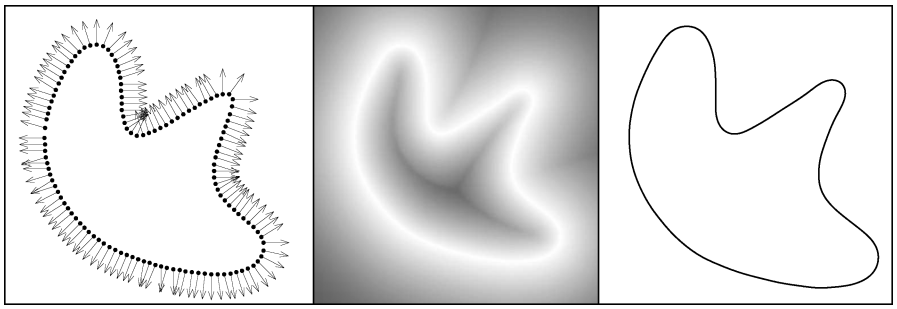

FIG. 1. Left, a set of points with approximate outside normals. Center, the cut function built by our algorithm from the points. The zero set of the cut function, which is the reconstructed curve, is shown on the right.

surface normal of F near s is also given. From this input, our interpolation scheme defines a surface passing near the sample points, represented implicitly as the zero set of a scalar function. Such implicit representations have many applications in computer graphics and have recently become important because of the popularity of point-based methods in modeling and simulation.

For each sample point $s \in S$, we define a globally smooth linear point function that approximates the *signed distance function* of F in the local neighborhood of s. These point functions are then combined using Gaussian weight functions yielding a three-dimensional function I, which we refer to as the cut function. The reconstructed surface U is given by the zero set of the cut function. Figure 1 shows a two-dimensional example.

Our definition of the cut function is based on a scattered data interpolation technique called *moving least squares* (MLS). MLS methods have been used to interpolate irregularly distributed function-value data and to build meshless interpolants in computational mechanics. One of the earliest MLS methods is the metric interpolation technique of Shepard [1968]. Lancaster and Salkauskas [1981] give an excellent description of the geometric and differential properties of MLS interpolants.

The MLS method analyzed in this article is not new; it is a variation of the implicit MLS surface defined by Shen et al. [2004]. We use the Gaussian function instead of the inverse distance as the weight function. The main contribution of this article is to introduce theoretical guarantees for MLS methods. We prove that the cut function I is a good approximation of the signed distance function of the sampled surface F. We also show that the reconstructed surface is geometrically and topologically correct. Our analysis also shows that the interpolation scheme is robust to noise in the input sample points when the noise is small compared to the smallest feature size of the sampled surface.

The Delaunay-based crust algorithm of Amenta and Bern [1999] was the first surface reconstruction algorithm that guaranteed a correct reconstruction for sufficiently dense sample sets. Our sampling and noise requirements are based on the local feature size function used in the analysis of the crust algorithm.

2. *Related Work*

2.1. IMPLICIT METHODS. Implicit methods that define the reconstructed surface as the zero set of a three-dimensional function are widely used in computer graphics.

Implicit methods are popular as they are easy to implement, scale well to large datasets, and are robust to noise in the input. Hoppe et al. [1992] provide one of the earliest algorithms, which locally estimates the signed distance function induced by the true surface sampled. Curless and Levoy [1996] developed an algorithm that is particularly effective for laser range data, comprising billions of point samples like the statue of David reconstructed by the Digital Michelangelo Project [Levoy et al. 2000]. Smooth surfaces can also be built by fitting globally supported basis functions to a point cloud. Turk and O'Brien [1999] show that a global smooth approximation can be obtained by fitting radial basis functions. Carr et al. [2001] adapt this radial basis function-fitting algorithm to large datasets using multipole expansions. MLS methods discussed in the next section are a subset of implicit methods.

2.2. MOVING LEAST SQUARES. Moving least squares belongs to a class of meshless interpolation methods used in computational mechanics that also includes partition-of-unity, kernel methods, and smoothed particle hydrodynamics. See the survey paper by Belytschko et al. [1996] for a comparison between these different formulations. In computer graphics, Ohtake et al. [2003] present a partition-of-unity method with a fast hierarchical evaluation scheme to compute surfaces from large datasets.

Cut functions defined as a weighted blend of point functions have been proposed before with different weight functions. Boissonnat and Cazals [2000] use natural neighbor coordinates derived from the Delaunay tetrahedralization of the sample points. The reconstructed surface interpolates the sample points and comes with provable guarantees. Shen et al. [2004] use the inverse squared distance as the weight function to build interpolating and approximating implicit surfaces from polygonal data.

A different approach to moving least squares is the nonlinear projection method originally proposed by Levin [2003]. A point-set surface is defined as the set of stationary points of a projection operator. This surface definition was first used by Alexa et al. [2003] for point-based modeling and rendering. Since then, the surface definition has been used for progressive point-set surfaces [Fleishman et al. 2003] and in PointShop3D [Pauly et al. 2003], a point-based modeling tool. Amenta and Kil [2004] give an explicit definition of point-set surfaces as the local minima of an energy function along the directions given by a vector field. Adamson and Alexa [2003] provide a simplified implicit surface definition for efficient ray tracing and define sampling conditions that guarantee a manifold reconstruction.

There has been some recent work on extending our result to handle adaptively sampled surfaces. Dey and Sun [2005] present a nonlinear projection method in which the width of the Gaussian weight functions varies with feature size. They prove reconstruction guarantees when sample spacing is proportional to local feature size.

2.3. DELAUNAY METHODS. Following the crust algorithm of Amenta and Bern [1999], there have been many Delaunay-based algorithms for surface reconstruction with provable guarantees. Amenta et al. [2002] present the cocone algorithm, which is much simpler than the crust, and prove that the reconstructed surface is homeomorphic to the original surface. The powercrust algorithm of Amenta et al. [2001] uses weighted Delaunay triangulations to avoid the manifold extraction step of the crust and cocone algorithms. The robust cocone algorithm of Dey and

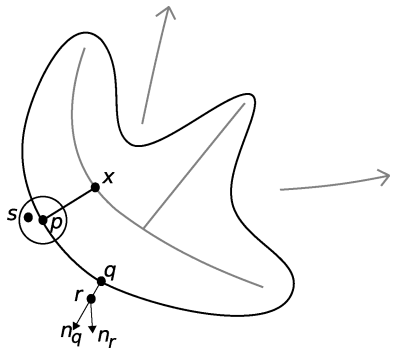

FIG. 2. A closed curve along with its medial axis. The local feature size of p is the distance to the closest point x on the medial axis.

Goswami [2004] guarantees a correct reconstruction for noisy point data. Delaunay-based algorithms do not require sample normals and can adapt well to changes in sample spacing. However, these algorithms build surfaces that interpolate (a subset of) the sample points and a mesh-smoothing step is often necessary for noisy data.

2.4. SIGNED DISTANCE FUNCTIONS. Signed distance functions of surfaces are useful in their own right. Level-set methods that have been used in surface reconstruction [Zhao et al. 2001], physical modeling of fluids, and in many other areas, rely on signed-distance functions to implicitly maintain moving surfaces. See the books by Sethian [1999] and Osher and Fedkiw [2003] for an introduction to level-set methods. Mitra et al. [2004] use approximation of signed-distance functions to align overlapping surfaces. The cut function constructed by the MLS interpolation scheme is a good approximation to the signed-distance function.

2.5. CONTOURING ALGORITHMS. Meshes that approximate the sampled surface can be built by contouring the zero set of the implicit function defined by our algorithm. The marching cubes [Lorensen and Cline 1987] algorithm is widely used in computer graphics for contouring level sets of implicit functions. There has been some recent work on contouring algorithms with theoretical guarantees. Boissonnat and Oudot [2003] give a Delaunay-based contouring algorithm that guarantees good quality triangles in the reconstructed surface. Boissonnat et al. [2004] present a contouring algorithm with guarantees on the topology of the reconstructed triangulation. The contouring algorithm developed by Plantiga and Vegter [2004] uses interval arithmetic to extract properties of the cut function and produces a triangulation isotopic to the zero set of the cut function.

3. *Sampling Requirements*

Our sampling requirements are based on the *local feature size* (lfs) function proposed by Amenta and Bern [1999]. For a point $p \in F$, $\text{lfs}(p)$ is defined as the distance from p to the nearest point x of the medial axis of F as shown in Figure 2. Our theoretical guarantees require sampling proportional to the smallest local feature size of F. As F is a smooth manifold, for each point $p \in F$, $\text{lfs}(p) > 0$. Assume that the dataset has been scaled such that the lfs of any point on F is at

least 1. We require that, for each point $p \in F$, the distance from p to its closest sample point s is less than ϵ, as shown in Figure 2.

We require the amount of noise in the samples to be small compared to the smallest feature size of the sampled surface. For each sample r, the distance to its closest surface point q should be less than ϵ^2 as shown in Figure 2. Moreover, the angle between the normal $\vec{n}_r$ of r and the normal $\vec{n}_q$ of q should be less than ϵ.

Arbitrary oversampling in one region of the surface can distort the value of the cut function in other parts of the surface. As this rarely happens in practice, we require that local changes in the sampling density are bounded. Let α_p be the number of samples inside a ball of radius ϵ, centered at a point p. If $\alpha_p > 0$, the number of samples inside a ball at radius 2ϵ at p should be less than 8α. The results in this article hold true for values of $\epsilon \leq 1/50$.

For a given surface F, our sampling requirements impose an upper bound on the amount of noise and the sample spacing required to reconstruct F. These upper bounds depend on the smallest feature size of F. To reconstruct a surface with feature size 1, the distance from each surface point to its nearest sample should be less than $1/50$, and the distance from each sample point to the surface should be less than $1/2500$. Errors in the sample normals should be less than $1/50$. The small value of ϵ is probably an artifact of our proof techniques. We found that the MLS function defined here works well for much larger values of ϵ in practice.

4. *Surface Definition*

Let $s_i \in S$ be the sample points in the input dataset that lie near the surface F. Let $\vec{n}_i$ be an approximate outside normal of sample s_i. In practice, the normal of s_i is obtained by local least-squares fitting of a plane to the sample points in the neighborhood around s_i. Mitra et al. [2004] analyze the least-squares method for normal estimation and present an algorithm for choosing an optimal neighborhood around each sample point.

For each sample point $s_i \in S$, the point function $P_i(x)$ is the signed distance from x to the tangent plane at s_i, $P_i(x) = (x - s_i) \cdot \vec{n}_i$. The cut function I is a weighted average of the point functions.

$$I(x) = \sum_{s_i \in S} \frac{W_i(x)}{\sum_{s_j \in S} W_j(x)} ((x - s_i) \cdot \vec{n}_i).$$

We use Gaussian functions, $W_i(x) = e^{-\|x - s_i\|^2/\epsilon^2}/a_i$, in computing the weighted average of the point functions. Here ϵ is the parameter defined in our sampling requirements and a_i is the number of sample points inside a ball of radius ϵ centered at s_i, including s_i itself. The number a_i normalizes for oversampling near s_i.

As our results will show, the accuracy of the reconstructed surface is proportional to ϵ. For a given set of sample points, the requirements discussed in Section 3 impose an upper bound on ϵ. In practice, the parameter ϵ is typically computed from the properties of the physical device or the algorithm used to generate the sample points and their normals.

The cut function is the best least-squares fit to the point functions in the following sense: at point x, each sample s_i votes for the value of the global function to be $P_i(x)$ with a weight $W_i(x)$; setting the cut function $I(x)$ to the weighted average of these point functions minimizes the weighted least-squares error in the estimate of $I(x)$.

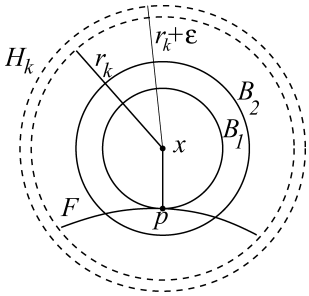

FIG. 3. For a point x, p is the closest point to x on the surface. The space outside the ball $B_2(x)$ is divided into spherical shells of width ϵ. H_k is the shell bounded by spheres of radius r_k and $r_k + \epsilon$.

5. *Geometric Properties*

To prove that the cut function converges to the signed-distance function of F, it is convenient to define an error function $E(x)$ that measures the difference between the cut function computed by the MLS algorithm and the signed-distance function $\phi(x)$. This error function $E(x)$ is given by,

$$E(x) = I(x) - \phi(x) = \sum_{s_i \in S} \frac{W_i(x)}{\sum_{s_j \in S} W_j(x)} (P_i(x) - \phi(x)) = \sum_{s_i \in S} \frac{W_i(x)}{\sum_{s_j \in S} W_j(x)} \delta_i(x). \tag{1}$$

The function $\delta_i(x)$, defined in Equation (1), measures the error in the point function of sample s_i. Our analysis of the cut function has two main ideas: first, the exponential decay of the Gaussian weight functions means that the cut function is mostly determined by samples inside $B_2(x)$ and, second, the cut function converges to the signed-distance function because the error functions associated with sample points inside $B_2(x)$ converge to zero as ϵ goes to zero.

Consider a point x shown in Figure 3 whose closest point on the surface is p. The vector $\vec{xp}$ is parallel to the surface normal of p and $\|\vec{xp}\| = |\phi(x)|$, where $\phi(x)$ is the signed-distance function of F evaluated at x. Let $B_1(x)$, $B_2(x)$ be two balls centered at point x. The radius of $B_1(x)$ is $|\phi(x)|$ and $B_2(x)$ is a slightly larger ball whose radius is $|\phi(x)| + \epsilon$ as shown in Figure 3.

To prove our results we separate the contributions of sample points inside $B_2(x)$ and outside $B_2(x)$ to the error function. Let $\xi(x) = \sum_{s_i \in S} \delta_i(x) W_i(x)$ be the weighted combination of error functions, and define $W(x) = \sum_{s_i \in S} W_i(x)$ to be the sum of all weight functions at x. Let $W_{\text{in}}(x)$ be the sum of weights of all sample points inside $B_2(x)$, and let $W_{\text{out}}(x)$ be the weight of all samples outside $B_2(x)$. Similarly, let $E_{\text{in}}(x)$, $E_{\text{out}}(x)$ be the contributions to the error function $E(x)$, and let $\xi_{\text{in}}(x)$, $\xi_{\text{out}}(x)$ be the contributions to $\xi(x)$ by samples inside and outside $B_2(x)$.

Let F_{out} be the outside ϵ-offset surface of F that is obtained by moving each point p on F along the normal at p by a distance ϵ. Similarly, let F_{in} be the inside ϵ-offset surface of F. Dey and Goswami [2004] prove that the offset surfaces have the same topology as F when ϵ is small relative to the lfs of each point on the surface. The ϵ-neighborhood is the region bounded by the inside and the outside offset surfaces; for any point x inside the ϵ-neighborhood, $|\phi(x)| < \epsilon$. In Section 5.1, we study the properties of the cut function for points outside the ϵ-neighborhood and prove that the cut function is nonzero outside the ϵ-neighborhood of F (Theorem 7).

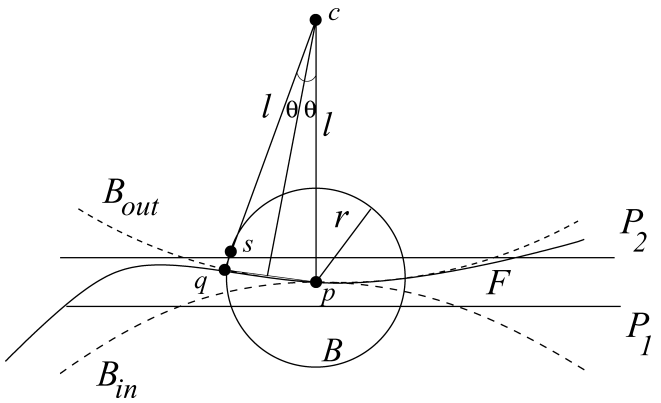

FIG. 4. The surface inside a ball B of radius r has to be outside the medial balls B_{in} and B_{out}. As a result, all samples in B are between two planes P_1 and P_2 that are at a distance of $O(r^2 + \epsilon^2)$ from p.

This means that the reconstructed surface is inside the ϵ-neighborhood of F. To prove that the reconstructed surface is a manifold, we analyze the gradient of the cut function for points inside the ϵ-neighborhood in Section 5.2. These geometric results will be used in Section 6 to show that U is isotopic to F.

We begin by proving some useful geometric properties of the surface and surface normals. Amenta and Bern [1999] prove the following Lipschitz condition on the surface normal with respect to the local feature size. As we assume that for each point $p \in F$, $\text{lfs}(p) \geq 1$, we can state the Lipschitz condition in terms of the distance between two points.

THEOREM 1. *For points p, q on the surface F with $d(p, q) \leq r$, for any $r < 1/3$, the angle between the normals at p and q is at most $r/(1 - 3r)$ radians.*

Consider a small ball B centered at a point $p \in F$ as shown in Figure 4. In the following lemma, we show that the surface inside B lies between two planes close to the tangent plane of p.

LEMMA 2. *For a point $p \in F$, let B be a ball of radius $r < 1/4$, centered at p. The sample points inside B lie between two planes P_1, P_2, parallel to the tangent plane at p. The distance from p to P_1, P_2 is less than $(r + \epsilon^2)^2/2 + \epsilon^2$.*

PROOF. Consider sample point $s \in B$ whose closest point on F is q. Without loss of generality, assume that s is above the tangent plane at p as shown in Figure 4. Then, $d(p, q) \leq d(p, s) + d(s, q) \leq r + d(s, q)$. As point q is on the surface, it has to be outside the medial ball B_{out} of radius $l \geq 1$. Hence the distance from q to the tangent plane at p is less than $l(1 - \cos 2\theta) = 2l \sin^2 \theta \leq d^2(p, q)/2$. From the noise conditions in our sampling requirements, $d(s, q) \leq \epsilon^2$. Therefore the distance from s to the tangent plane at p is less than $d^2(p, q)/2 + \epsilon^2 = (r + \epsilon^2)^2/2 + \epsilon^2$. □

Partition the space outside $B_2(x)$ into spherical shells of width ϵ, as shown in Figure 3. Let H_k be the region between balls of radius r_k and $r_k + \epsilon$. We will sum over the spherical shells starting at $B_2(x)$ to prove an upper bound on the error in the cut function due to samples outside $B_2(x)$. In the following lemma, we prove an upper bound on the weights of sample points inside each shell.

LEMMA 3. *For a ball B of radius $\frac{\epsilon}{2}$, $\sum_{s_i \in B} \frac{1}{a_i} \leq 1$.*

PROOF. If B is empty, we are done; assume that B contains $\alpha > 0$ samples. Consider a sample point $s_i \in B$. Since all sample points in B are inside a ball of radius ϵ centered at s_i, $a_i \geq \alpha$. So an upper bound on the weight of all sample points inside B is given by $\sum_{s_i \in B} \frac{1}{a_i} \leq \alpha \frac{1}{\alpha} \leq 1$. □

LEMMA 4. *Let H_k be a spherical shell of width ϵ, centered at point x, such that the radius of the smaller sphere surrounding H_k is $r_k > 4\epsilon$. Then, for samples $s_i \in H_k$, $\sum_{s_i \in H_k} \frac{1}{a_i} < 300 \frac{r_k^2}{\epsilon^2}$.*

PROOF. Let C be the smallest number of spheres of radius $\epsilon/2$ that cover H_k. Consider a covering of H_k with axis-parallel cubes of size $\epsilon/\sqrt{3}$. Any cube that intersects H_k is inside a slightly larger shell bounded by spheres of radius $r_k + 2\epsilon$ and $r_k - \epsilon$, centered at x. So the number of cubes that cover H_k is less than $36\sqrt{3}\pi\epsilon(r_k^2 + r_k\epsilon + \epsilon^2)/\epsilon^3$. Any cube in this grid is covered by a sphere of radius $\epsilon/2$. Applying Lemma 3 to each sphere, $\sum_{s_i \in H_k} \frac{1}{a_i} \leq C \leq 36\sqrt{3}\pi(r_k^2 + r_k\epsilon + \epsilon^2)/\epsilon^2$. As $r_k > 4\epsilon$, we can simplify the above expression to get,

$$\sum_{s_i \in H_k} \frac{1}{a_i} \leq 36\sqrt{3}\pi \left(r_k^2 + r_k\epsilon + \epsilon^2\right)/\epsilon^2 < 300\frac{r_k^2}{\epsilon^2}. \quad \square$$

5.1. OUTSIDE THE ϵ-NEIGHBORHOOD. In this section, we analyze the error function $E(x)$ for points outside the ϵ-neighborhood. We prove that the cut function is mostly determined by samples inside $B_2(x)$ and that the cut function is nonzero outside the ϵ-neighborhood. This result has practical significance as it shows that a good approximation to the cut function can be efficiently evaluated from sample points inside $B_2(x)$.

In the following lemma, we show that for $s_i \in B_2(x)$, $P_i(x)$ is close to $\phi(x)$. To state this result for points in the inside and outside offset regions, we define the sign function of F as $\mu(x) = \frac{\phi(x)}{|\phi(x)|}$. For x outside F_{out}, $\mu(x) = 1$, and for x inside F_{in}, $\mu(x) = -1$.

LEMMA 5. *Let x be a point outside the ϵ-neighborhood. Let $\delta_i(x)$ be the error in the point function of sample $s_i \in B_2(x)$ evaluated at x. Then, $\mu(x)\delta_i(x) \leq 4\epsilon$, and, $\mu(x)\delta_i(x) \geq -(8\epsilon\mu(x)\phi(x) + 20\epsilon^2)$.*

PROOF. Let p be a closest point to x on the surface. Therefore, $d(x, p) = \mu(x)\phi(x)$. Since sample point s_i is inside $B_2(x)$,

$$\begin{aligned} \mu(x)P_i(x) &\leq d(x, s_i) \\ &\leq \mu(x)\phi(x) + 4\epsilon. \\ \mu(x)\delta_i(x) &\leq 4\epsilon. \end{aligned}$$

Let p' be the closest point to s_i on the surface F as shown in Figure 5. Let B_m be the medial ball touching p' on the side of F opposite x, and let l be the radius of B_m. Let θ be the angle between xp' and the normal at p'. The distance between x and the center of B_m is given by

$$d^2(x, q) = (d(x, p')\cos\theta + l)^2 + d^2(x, p')\sin^2\theta.$$

The medial ball B_m cannot intersect $B_1(x)$ which is contained in a medial ball on the opposite side of the surface. Hence the sum of their radii should be less than

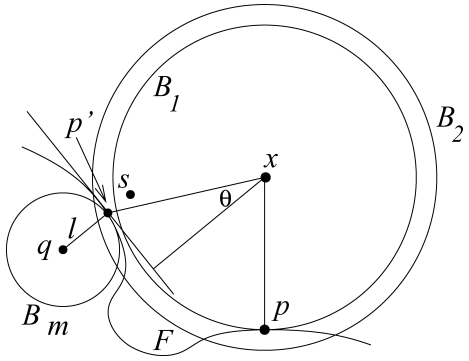

FIG. 5. Sample point s is inside $B_2(x)$ and p' is the point closest to s on F. B_m is a medial ball touching p' on the side of F opposite x.

the distance between their centers.

$$\begin{aligned}(l + d(x, p))^2 &\leq (d(x, p')\cos\theta + l)^2 + d^2(x, p')\sin^2\theta.\\ \cos\theta &\geq \frac{1}{2ld(x, p')}(2ld(x, p) - (d^2(x, p') - d^2(x, p))).\end{aligned}$$

From the sampling conditions, $d(x, s_i) \geq d(x, p') - \epsilon^2$, and the angle between the normal at s_i and the surface normal at p' is less than ϵ. As $d(x, p') \geq \epsilon$, the angle between xs_i and xp' is less than $\arcsin(\epsilon^2/\epsilon) < 2\epsilon$. So the angle between xs_i and the normal at s_i is at most $\theta + 2\epsilon + \epsilon = \theta + 3\epsilon$. Using standard trigonometric formulas, it is easy to show that, $\cos(\theta + 3\epsilon) \geq \cos\theta - 3\epsilon$.

$$\begin{aligned}\mu(x)P_i(x) &\geq d(x, s_i)\cos(\theta + 3\epsilon)\\ &\geq (d(x, p') - \epsilon^2)\cdot\left(\frac{2ld(x, p) - (d^2(x, p') - d^2(x, p))^2}{2ld(x, p')} - 3\epsilon\right)\\ &\geq \left(1 - \frac{\epsilon^2}{d(x, p')}\right)(|\phi(x)| - \frac{1}{2l}(d^2(x, p') - |\phi(x)|^2)) - 3\epsilon\, d(x, p').\end{aligned}$$

Since x is outside the ϵ-neighborhood and p' is inside $B_2(x)$, $\epsilon \leq d(x, p') \leq |\phi(x)| + 4\epsilon$. From the local feature-size assumption, $l \geq 1$. Substituting these bounds into the previous equation, we have

$$\mu(x)\delta_i(x) \geq -(8\epsilon\mu(x)\phi(x) + 20\epsilon^2). \quad \square$$

In the following two results, we show that the points outside $B_2(x)$ have little effect on the value of $I(x)$. We will use a small constant $c_1 = 0.001$ to state these results.

LEMMA 6. *Let x be a point outside the ϵ-neighborhood. Let $W_{\text{out}}(x)$ be the total weight of sample points outside $B_2(x)$. Then, $\frac{W_{\text{out}}(x)}{W(x)} < c_1$, and $|E_{out}(x)| < c_1\epsilon$.*

PROOF. As shown in Figure 3, consider the division of space outside $B_2(x)$ into spherical shells of width ϵ starting with $B_2(x)$ of radius $r_0 = |\phi(x)| + 4\epsilon$. The value of the Gaussian function associated with each sample inside shell H_k at x is

at most $e^{-r_k^2/\epsilon^2}$. Using the bound on the weight of samples in H_k from Lemma 4,

$$W_{\text{out}}(x) \leq \frac{300}{\epsilon^2} \sum_{k=0}^{\infty} r_k^2 e^{-r_k^2/\epsilon^2} \leq \frac{300}{\epsilon^2} \sum_{k=0}^{\infty} r_k^2 e^{-(r_0 r_k)/\epsilon^2}. \tag{2}$$

Here r_k=$r_0 + k\epsilon$ is the radius of the smaller sphere bounding H_k. The summation in Equation (2) is a geometric series with a common ratio $e^{-r_0/\epsilon} < 0.01$ that has a closed form solution. An upper bound is given by

$$W_{\text{out}}(x) \leq 450 \frac{r_0^2}{\epsilon^2} e^{-r_0^2/\epsilon^2}.$$

The sum of weights of sample points inside $B_2(x)$ is a lower bound on $W(x)$. Let B_ϵ be a ball of radius ϵ centered at p. From the sampling requirements, B_ϵ contains $\alpha \geq 1$ samples, and a ball of radius 2ϵ, centered at p, contains at most 8α samples. So the oversampling factor associated with $s_i \in B_\epsilon$ is $\frac{1}{a_i} \geq \frac{1}{8\alpha}$. Therefore

$$W(x) > W_2(x) \geq \sum_{s_i \in B_\epsilon} \frac{1}{a_i} e^{-(|\phi(x)|+\epsilon)^2/\epsilon^2} \geq \frac{\alpha}{8\alpha} e^{-(|\phi(x)|+\epsilon)^2/\epsilon^2} = \frac{1}{8} e^{-(|\phi(x)|+\epsilon)^2/\epsilon^2}. \tag{3}$$

This lower bound is the only result that requires these uniformity conditions. By adding sample points right outside B_ϵ, we can arbitrarily reduce the oversampling factors for each sample point $s_i \in B_\epsilon$.

The error functions of sample points outside B_ϵ might have a large value when evaluated at x. Therefore, such oversampling can distort the value of the cut function at x. Note that the lower bound in Equation (3) is also valid inside the ϵ-neighborhood. From Equation (3), an upper bound on the ratio of the outside weights to the total weight is given by

$$\frac{W_{\text{out}}(x)}{W(x)} \leq 3600 \frac{r_0^2}{\epsilon^2} e^{-(r_0^2-(|\phi(x)|+\epsilon)^2)/\epsilon^2} = 3600 \frac{r_0^2}{\epsilon^2} e^{-3\epsilon(2|\phi(x)|+5\epsilon)/\epsilon^2}.$$

For $|\phi(x)| \geq \epsilon$, the upper bound on $\frac{W_{\text{out}}(x)}{W(x)}$ is a monotonically decreasing function of $|\phi(x)|$. The maximum value is obtained for $|\phi(x)| = \epsilon$ and $r_0 = \epsilon + 4\epsilon = 5\epsilon$.

$$\frac{W_{\text{out}}(x)}{W(x)} \leq 3600 \frac{25\epsilon^2}{\epsilon^2} e^{-21} < c_1.$$

We will now prove a similar bound on $|E_{\text{out}}(x)|$. Recall that $\delta_i(x)$ in the error in the point function associated with sample point s_i when evaluated at x, and $\xi_{\text{out}}(x)$ is the weighted sum of the error functions for all sample points outside $B_2(x)$. Consider sample $s_i \in H_k$ for $k \geq 0$. The point function of s_i is $|P_i(x)| \leq \|x - s_i\|$ and $|\phi(x)| < \|x - s_i\|$. Hence, $|\delta_i(x)| \leq |\phi(x)| + \|x - s_i\| < 2\|x - s_i\|$.

$$|\xi_{\text{out}}(x)| \leq \sum_{s_i \notin B_2(x)} |\delta_i(x)| W_i(x) < 2 \sum_{s_i \notin B_2(x)} \|x - s_i\| W_i(x). \tag{4}$$

For $\|x - s_i\| \geq r_0$, the value of $\|x - s_i\| e^{-\|x-s_i\|^2/\epsilon^2}$ decreases as $\|x - s_i\|$ increases.

Hence for each $s_i \in H_k$, $|\delta_i(x)|W_i(x) \leq 2r_k e^{-r_k^2/\epsilon^2}/a_i$.

$$|\xi_{\text{out}}(x)| < \frac{600}{\epsilon^2} \sum_{k=0}^{\infty} r_k^3 e^{-r_k^2/\epsilon^2}.$$

Just like Equation (2), an upper bound of the summation in this equation is given by

$$|\xi_{\text{out}}(x)| < \frac{900}{\epsilon^2} r_0^3 e^{-r_0^2/\epsilon^2}.$$

Substituting the lower bound of $W(x)$ from Equation (3), we have

$$\frac{|\xi_{\text{out}}(x)|}{W(x)} < \frac{7200}{\epsilon^2} r_0^3 e^{-(r_0^2-(|\phi(x)|+\epsilon)^2)/\epsilon^2} = \frac{7200}{\epsilon^2} r_0^3 e^{-3\epsilon(2|\phi(x)|+5\epsilon)/\epsilon^2}. \tag{5}$$

The value of $E_{\text{out}}(x)$ is maximized for $r_0 = 5\epsilon$. Hence,

$$|E_{\text{out}}(x)| = \frac{|\xi_{\text{out}}(x)|}{W(x)} < \frac{7200}{\epsilon^2}(125\epsilon^3)e^{-21} < c_1\epsilon. \quad \square$$

We now have all the tools required to prove that the cut function $I(x)$ is nonzero outside the ϵ-neighborhood.

THEOREM 7. *For each point x outside F_{out}, $I(x) > 0$ and for each point y inside F_{in}, $I(y) < 0$.*

PROOF. Consider point x outside F_{out}. The cut function at x is given by, $I(x) = \phi(x) + E_{\text{in}}(x) + E_{\text{out}}(x)$. Lemma 5 gives us a lower bound on $E_{\text{in}}(x)$.

$$\begin{aligned} E_{\text{in}}(x) &= \frac{1}{W(x)} \sum_{s_i \in B_2(x)} \delta_i(x) W_i(x) \\ &\geq \min\{\delta_i(x) | s_i \in B_2(x)\} \frac{W_{\text{in}}(x)}{W(x)} \\ &> -(8\epsilon\phi(x) + 20\epsilon^2). \end{aligned}$$

From Lemma 6, we know that $E_{\text{out}}(x) > -c_1\epsilon$. Adding the lower bounds on $E_{\text{in}}(x)$ and $E_{\text{out}}(x)$, we have

$$I(x) > \phi(x)(1 - 8\epsilon) - 20\epsilon^2 - c_1\epsilon.$$

As x is outside F_{out}, $\phi(x) \geq \epsilon$. It is easy to check that $I(x) > 0$ when $\epsilon \leq 1/50$. A similar argument proves that the cut function is negative at any point y inside F_{in}. $\square$

Theorem 7 proves that the cut function I does not have any spurious zero crossings far away from the sample points. Combining the results in Lemma 5 and Lemma 6, it is easy to show that the cut function converges to the signed-distance function as ϵ goes to zero.

$$\mu(x)I(x) \geq \mu(x)\phi(x)(1 - 8\epsilon) - 20\epsilon^2 - c_1\epsilon.$$

$$\mu(x)I(x) \leq \mu(x)\phi(x) + 4\epsilon + c_1\epsilon.$$

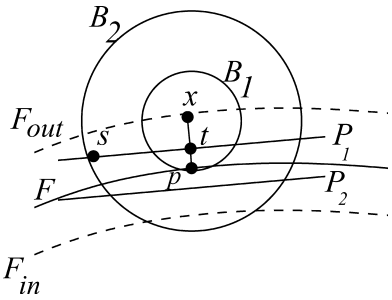

FIG. 6. For x in the ϵ-neighborhood, the sample points inside ball $B_2(x)$ are contained in a ball of radius 4ϵ, centered at p.

5.2. THE ϵ-NEIGHBORHOOD. In this section, we analyze the cut function for points inside the ϵ-neighborhood which contains the reconstructed surface. We prove that the reconstructed surface U is a smooth manifold that converges to the sampled surface as ϵ goes to zero. Since the point functions and the weight functions used in computing the cut function are all globally smooth, U is guaranteed to be smooth. We study the properties of the cut-function gradient to prove that U is a manifold. Based on the analysis of the gradient function, we also show that the normals of the reconstructed surface converge to the normals of F as ϵ goes to zero.

For x inside the ϵ-neighborhood, define $B_2(x)$ as a ball of radius $r_0 = \sqrt{(|\phi(x)| + \epsilon)^2 + 12\epsilon^2}$ centered at x. In the following lemma, we show that the sample points inside $B_2(x)$ are contained in a small ball centered at the point closest to x in F.

LEMMA 8. *Let x be a point that is inside the ϵ-neighborhood, and let p be the closest point to x in F. All sample points inside $B_2(x)$ are contained in a ball of radius 4ϵ, centered at p.*

PROOF. Let s be a sample point inside $B_2(x)$, and let P_1 be a plane parallel to the tangent plane at p and passing through s. The line segment xp intersects P_1 at point t, as shown in Figure 6. The distance from s to t is given by

$$d^2(s,t) = d^2(s,p) - d^2(p,t) = d^2(x,s) - d^2(x,t).$$

As s is inside $B_2(x)$, $d^2(x,s) \le (|\phi(x)| + \epsilon)^2 + 12\epsilon^2$,

$$\begin{aligned} d^2(s,p) - d^2(p,t) &\le (|\phi(x)| + \epsilon)^2 + 12\epsilon^2 - (|\phi(x)| - d(p,t))^2 \\ d^2(s,p) &\le 13\epsilon^2 + 2|\phi(x)|\epsilon + 2|\phi(x)|d(p,t) \\ &< 15\epsilon^2 + 2\epsilon\, d(p,t). \end{aligned} \tag{6}$$

Any sample point inside $B_2(x)$ is clearly inside a ball of radius 5ϵ centered at p. Therefore from Lemma 2, s is between two planes, P_1 and P_2, parallel to the tangent plane at p and at a distance $(5\epsilon + \epsilon^2)^2/2$ from p and $d(p,t) \le (5\epsilon + \epsilon^2)/2 + \epsilon^2 < 14\epsilon^2$. Substituting the bound on $d(p,t)$ into Equation (6), $d^2(s,p) < 15\epsilon^2 + 28\epsilon^3 < 16\epsilon^2$. □

In the following lemma, we prove an upper bound for the errors in the point functions of sample points near p.

LEMMA 9. *Consider a point x whose closest point on the surface F is p. Let $\vec{n}$ be the surface normal at p, and let B be a ball of radius $r \leq 1/4$ at p. For each sample point $s_i \in B$, the angle between the normal at s_i and $\vec{n}$ is less than $\Theta(r) = \frac{r+\epsilon^2}{1-3(r+\epsilon^2)} + \epsilon$. For each sample $s_i \in B$, $|\delta_i(x)| \leq |\phi(x)|\Theta(r)^2/2 + r\Theta(r) + (r+\epsilon^2)^2/2 + \epsilon^2$.*

PROOF. Let p_i be the point closest to s_i on F. Then, $d(p, p_i) \leq d(p, s_i) + d(s_i, p_i) \leq r + \epsilon^2$. From Theorem 1, the angle between the normal at p_i and the surface normal $\vec{n}$ at p is less than $\frac{r+\epsilon^2}{1-3(r+\epsilon^2)}$.

Let $\vec{n}_i$ be the normal associated with s_i. From the sampling conditions, we know that the angle between the normal of p_i and $\vec{n}_i$ is at most ϵ. So the angle between $\vec{n}_i$ and $\vec{n}$ is given by $\Theta(r) < \frac{r+\epsilon^2}{1-3(r+\epsilon^2)} + \epsilon$. Therefore $\vec{n}_i = \vec{n} + \vec{\rho}_i$, where $\|\vec{\rho}_i\| \leq \Theta(r)$.

$$\begin{aligned} \delta_i(x) &= \phi(x) - P_i(x) \\ &= \phi(x) - (x - s_i) \cdot \vec{n}_i \\ &= \phi(x) - (x - p) \cdot \vec{n}_i - (p - s_i) \cdot (\vec{n} + \vec{\rho}_i). \end{aligned} \tag{7}$$

Because p is the closest point to x on the surface, $(x - p)$ is parallel to $\vec{n}$ and $\|x - p\| = |\phi(x)|$.

$$|\phi(x) - (x - p) \cdot \vec{n}_i| \leq |\phi(x)|(1 - \cos\Theta(r)) \leq |\phi(x)|\Theta^2(r)/2.$$

Since sample s_i is inside B,

$$|(p - s_i) \cdot \vec{\rho}_i| \leq r\Theta(r).$$

From Lemma 2, the distance from each sample inside B to the tangent plane at p is at most

$$|(p - s_i) \cdot \vec{n}| \leq (r + \epsilon^2)^2/2 + \epsilon^2.$$

Substituting the upper bounds on the individual terms, Equation (7) gives the desired result.

$$\begin{aligned} |\delta_i(x)| &\leq |\phi(x) - (x - p) \cdot \vec{n}_i| + |(p - s_i) \cdot \vec{\rho}_i| + |(p - s_i) \cdot \vec{n}| \\ &\leq |\phi(x)|\Theta^2(r)/2 + r\Theta(r) + (r + \epsilon^2)^2/2 + \epsilon^2. \quad \square \end{aligned}$$

In Lemma 8, we proved that all samples inside $B_2(x)$ are contained in a small ball around the point closest to x on F. So the result in Lemma 9 gives us an upper bound on the error functions of all samples inside $B_2(x)$. In the following two results, we derive a tighter bound on the error function $E(x)$.

LEMMA 10. *For a point x inside the ϵ-neighborhood, $|E_{\text{in}}| \leq 30\epsilon^2$.*

PROOF. We will use the results in Lemma 8 and Lemma 9 to get the desired bound.

$$|E_{\text{in}}(x)| = \frac{|\xi_{\text{in}}(x)|}{W(x)} \leq \sum_{s_i \in B_2(x)} \frac{|\delta_i(x)|W_i(x)}{W(x)} \leq \max\{|\delta_i(x)| \mid s_i \in B_2(x)\}.$$

From Lemma 8, we know that each sample $s_i \in B_2(x)$ is inside a ball of radius 4ϵ around p, the point closest to x on F. From Lemma 9, we have

$$|\delta_i(x)| \leq |\phi(x)|\Theta^2(4\epsilon)/2 + 4\epsilon\Theta(4\epsilon) + (4\epsilon + \epsilon^2)^2/2 + \epsilon^2 < 30\epsilon^2. \quad \square$$

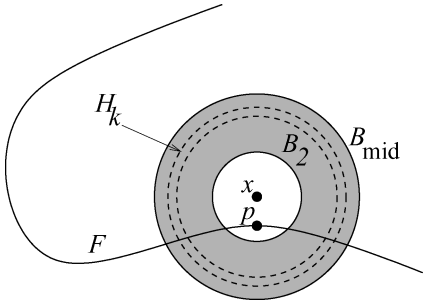

FIG. 7. When point x is inside the ϵ-neighborhood, all samples inside $B_{\text{mid}}(x)$ are near p, the point closest to x on F. As a result, the error in the point functions of samples inside $B_{\text{mid}}(x)$, evaluated at x, is small.

Note that the $O(\epsilon)$ bound on $|E_{\text{out}}(x)|$ obtained in Lemma 6 is also valid for points inside the ϵ-neighborhood. However, we can do better. Consider a ball $B_{\text{mid}}(x)$ of radius $r_{\text{mid}} = 0.125$, centered at point x, as shown in Figure 7. Note that r_{mid} is a fixed constant and does not depend on ϵ. All samples inside $B_{\text{mid}}(x)$ are near p, the point closest to x on F. As a result, the magnitude of error functions of samples inside $B_{\text{mid}}(x)$ is $O(r^2)$ from Lemma 8. Contrast this with the proof of Lemma 6 where we assumed that the error in all samples outside $B_2(x)$ is $O(r)$. This observation allows us to prove a better upper bound on $|E_{\text{out}}(x)|$. We first prove a result that improves the bound on the weight of samples inside a shell H_k contained in $B_{\text{mid}}(x)$.

LEMMA 11. *For a point x inside the ϵ-neighborhood, let H_k be a spherical shell centered at x that is outside $B_2(x)$ and inside $B_{\text{mid}}(x)$. The shell H_k is bounded by two spheres of radius r_k and $r_k + \epsilon$. Then, $\sum_{s_i \in H_k} \frac{1}{a_i} < 4\frac{r_k^3}{\epsilon^3}$.*

PROOF. Given in the appendix. □

LEMMA 12. *For a point x inside the ϵ-neighborhood, $|E_{\text{out}}(x)| < 4\epsilon^2$.*

PROOF. Like in the proof of Lemma 6, we compute the desired upper bound by summing over the contributions of samples inside shells H_k starting at $B_2(x)$. Let $\xi_1(x)$ and $\xi_2(x)$ be the contributions to $\xi_{\text{out}}(x)$ by samples inside $B_{\text{mid}}(x)$ and outside $B_{\text{mid}}(x)$, respectively. For x inside the ϵ-neighborhood, each sample in shell H_k, $r_k \leq r_{\text{mid}}$ is inside a ball of radius $r_k + 2\epsilon \leq r_{\text{mid}} + 2\epsilon < 1/4$, centered at p, the point closest to x on F. Hence, lemma 9 gives us a bound on $\delta_i(x)$. Using the inequality $\sqrt{12}\epsilon \leq r_0 \leq r_k \leq r_{\text{mid}}$,

$$\Theta(r_k + 2\epsilon) \leq \frac{r_k + 2\epsilon + \epsilon^2}{1 - 3(r_k + 2\epsilon + \epsilon^2)} \leq \frac{r_k(1 + 2/\sqrt{12} + \epsilon/\sqrt{12})}{1 - 3(r_{\text{mid}} + 2/50 + 1/2500)} \approx 3.06 r_k, \tag{8}$$

and,

$$\begin{aligned} |\delta_i(x)| &\leq |\phi(x)|\Theta^2(r_k + 2\epsilon)/2 + (r_k + 2\epsilon)\Theta(r_k + 2\epsilon) + (r_k + 2\epsilon + \epsilon^2)^2/2 + \epsilon^2 \\ &\approx 6.25 r_k^2 < 7 r_k^2. \end{aligned} \tag{9}$$

Substituting the upper bound on the weights of samples in shells H_k contained in $B_{\text{mid}}(x)$ from Lemma 11,

$$|\xi_1(x)| \leq \frac{42}{\epsilon^3} \sum_{k=0}^{r_k \leq r_{\text{mid}}} r_k^5 e^{-r_k^2/\epsilon^2} < \frac{42}{\epsilon^3} \sum_{k=0}^{\infty} r_k^5 e^{-r_0 r_k/\epsilon^2} \leq \frac{63}{\epsilon^3} r_0^5 e^{-r_0^2/\epsilon^2}. \tag{10}$$

Using the lower bound on $W(x)$ from Equation (3),

$$\frac{|\xi_1(x)|}{W(x)} < \frac{504}{\epsilon^3} r_0^5 e^{-(r_0^2-(|\phi(x)|+\epsilon)^2/\epsilon^2)} < \frac{504}{\epsilon^3} r_0^5 e^{-12}. \tag{11}$$

For samples outside $B_{\text{mid}}(x)$, we revert to the bound obtained in Lemma 6 on the error function associated with each sample. From Equation (4),

$$|\xi_2(x)| \leq \sum_{s_i \notin B_{\text{mid}}(x)} |\delta_i(x)| W_i(x) \leq 2 \sum_{s_i \notin B_{\text{mid}}(x)} \|x - s_i\| W_i(x).$$

The expression for $|\xi_2(x)|$ is the same as the expression for $|\xi_{\text{out}}(x)|$ in the proof of Lemma 6 except that the summation begins at r_{mid} instead of r_{out}. Hence from Equation (5),

$$\frac{|\xi_2(x)|}{W(x)} \leq \frac{7200}{\epsilon^2} r_{\text{mid}}^3 e^{-(r_{\text{mid}}^2-(|\phi(x)|+\epsilon)^2)/\epsilon^2} \leq \frac{7200e^4}{\epsilon^2} r_{\text{mid}}^3 e^{-r_{\text{mid}}^2/\epsilon^2}. \tag{12}$$

Note that the expression in Equation (12) is $o(\epsilon^2)$. For x inside the ϵ-neighborhood , $r_0 \leq \sqrt{(\epsilon+\epsilon)^2 + 12\epsilon^2} = 4\epsilon$. We get the desired result by adding the upper bounds in Equation (11) and Equation (12).

$$|E_{\text{out}}(x)| \leq \frac{504}{\epsilon^3}(4\epsilon)^5 e^{-12} + \frac{7200e^4}{\epsilon^2} r_{\text{mid}}^3 e^{-r_{\text{mid}}^2/\epsilon^2} < 4\epsilon^2. \quad \square$$

In the following lemmas, we prove an upper bound on the error in the cut function inside the ϵ-neighborhood which shows that the Hausdorff distance between F and the reconstructed surface U is $O(\epsilon^2)$.

THEOREM 13. *For a point x inside the ϵ-neighborhood, $|E(x)| < 34\epsilon^2$.*

PROOF. Adding the bounds on $|E_{\text{in}}(x)|$ and $|E_{\text{out}}(x)|$ in Lemma 10 and Lemma 12 gives the desired result.

$$|E(x)| \leq |E_{\text{in}}(x)| + |E_{\text{out}}(x)| < 30\epsilon^2 + 4\epsilon^2 = 34\epsilon^2. \quad \square$$

THEOREM 14. *For a point $x \in U$, let p be the closest point in F. Then $d(x, p) < 34\epsilon^2$.*

PROOF. Since $x \in U$, $I(x) = 0$. Point x is inside the ϵ-neighborhood from Theorem 7. Applying the result in Theorem 13, the error function at x, $|E(x)| < 34\epsilon^2$. Therefore, $d(x, p) = |\phi(x)| \leq |I(x)| + |E(x)| < 34\epsilon^2$. $\square$

THEOREM 15. *For a point $p \in F$, let q be the closest point in U. Then, $d(p, q) \leq 34\epsilon^2$.*

PROOF. If $I(p) = 0$, we are done; assume without loss of generality that $I(p) < 0$. Let t be the point on the outside normal of p at a distance of $34\epsilon^2$ from p.

From Theorem 13, $|I(t)| \geq |\phi(t)| - |E(x)| > d(p,t) - 34\epsilon^2 = 0$. As the cut function I is continuous, there is a point s on pt at which $I(s) = 0$ and $d(p,s) < 34\epsilon^2$. Since q is the closest point to p in U, $d(p,q) \leq d(p,s) < 34\epsilon^2$. □

5.3. GRADIENT. The gradient of the cut function can be written as $\nabla I(x) = \nabla\phi(x) + \nabla E(x)$. The gradient of the signed-distance function is $\nabla\phi(x) = \vec{n}$, where $\vec{n}$ is the surface normal of p, the point closest to x on F. The expression for the gradient of the error function can be simplified to

$$\nabla E(x) = \sum_{s_i \in S} \frac{(\vec{n} - \vec{n}_i) W_i(x)}{W(x)} + \sum_{s_i, s_j \in S} \frac{2 W_i(x) W_j(x) \delta_i(x) (s_i - s_j)}{\epsilon^2 W^2(x)}. \quad (13)$$

We separate the contributions by samples inside and outside $B_2(x)$ to the gradient of the error function.

$$\nabla E_{\text{in}}(x) = \sum_{s_i \in B_2(x)} \frac{(\vec{n} - \vec{n}_i) W_i(x)}{W(x)} + \sum_{s_i, s_j \in B_2(x)} \frac{2 W_i(x) W_j(x) \delta_i(x) (s_i - s_j)}{\epsilon^2 W^2(x)}, \quad (14)$$

and,

$$\nabla E_{\text{out}}(x) = \sum_{s_i \notin B_2(x)} \frac{(\vec{n} - \vec{n}_i) W_i(x)}{W(x)} + \sum_{s_i \notin B_2(x) \vee s_j \notin B_2(x)} \frac{2 W_i(x) W_j(x) \delta_i(x) (s_i - s_j)}{\epsilon^2 W^2(x)}. \quad (15)$$

LEMMA 16. *Let x be a point in the ϵ-neighborhood of F, and let p be the point on F closest to x. Let $\vec{n}$ be the normal of p. Then , $\|\nabla E_{\text{in}}(x)\| < 486\epsilon$, and $|\vec{n} \cdot \nabla E_{\text{in}}(x)| < 1158\epsilon^2$.*

PROOF. From Equation (14),

$$\begin{aligned} \|\nabla E_{\text{in}}(x)\| &\leq \sum_{s_i \in S} \frac{\|\vec{n} - \vec{n}_i\| W_i(x)}{W(x)} + \sum_{s_i, s_j \in B_2(x)} \frac{2 W_i(x) W_j(x) |\delta_i(x)| \, \|s_i - s_j\|}{\epsilon^2 W^2(x)} \\ &\leq \max\{\|\vec{n} - \vec{n}_i\| \mid s_i \in B_2(x)\} \\ &\quad + \frac{2}{\epsilon^2} \max\{|\delta_i(x)| \|s_i - s_j\| \mid s_i, s_j \in B_2(x)\}. \end{aligned}$$

From Lemma 9, $\|\vec{n} - \vec{n}_i\| \leq \Theta(4\epsilon) < 6\epsilon$. From the proof of Lemma 10, the error function of each sample $s_i \in B_2(x)$, $|\delta_i(x)| < 30\epsilon^2$ and for samples $s_i, s_j \in B_2(x)$, $\|s_i - s_j\| \leq 8\epsilon$. Hence,

$$\|\nabla E_{\text{in}}(x)\| < 6\epsilon + 480\epsilon < 486\epsilon.$$

Consider $\nabla E_{\text{in}}(x)$ projected onto the normal vector $\vec{n}$.

$$\begin{aligned} \vec{n} \cdot \nabla E_{\text{in}}(x) &\leq \max\{|\vec{n} \cdot (\vec{n} - \vec{n}_i)| \mid s_i \in B_2(x)\} \\ &\quad + \frac{2}{\epsilon^2} \max\{|\delta_i(x) \vec{n} \cdot (s_i - s_j)| \mid s_i, s_j \in B_2(x)|\}. \end{aligned}$$

Since the angle between $\vec{n}$ and $\vec{n}_i$ is less than $\Theta(4\epsilon) \leq 6\epsilon$, $\vec{n} \cdot (\vec{n} - \vec{n}_i) = 1 - \cos 6\epsilon \leq 18\epsilon^2$. From Lemma 2, the distance from all samples inside $B_2(x)$ to the tangent plane at p is at most $(4\epsilon + \epsilon^2)^2/2 + \epsilon^2$. Hence $|\vec{n} \cdot (s_i - s_j)| \leq (4\epsilon + \epsilon^2)^2 + 2\epsilon^2 < 19\epsilon^2$. Substituting these upper bounds we get,

$$\vec{n} \cdot \nabla E_{\text{in}}(x) < 18\epsilon^2 + 1140\epsilon^2 < 1158\epsilon^2. \quad \square$$

The following lemma shows that the samples outside $B_2(x)$ have little affect on the gradient of the cut function. The proof is similar to the proof of Lemma 12 and is given in the appendix.

LEMMA 17. *For each point x inside the ϵ-neighborhood, $\|\nabla E_{\text{out}}(x)\| < 146\epsilon$ and $|\vec{n} \cdot \nabla E_{\text{out}}(x)| < 496\epsilon^2$.*

PROOF. Given in the appendix. □

THEOREM 18. *For a point x inside the ϵ-neighborhood, let $\vec{n}$ be the surface normal of p, the point closest to x on F. Then, $\vec{n} \cdot \nabla I(x) > 0$.*

PROOF. From the definition of the error function,

$$\vec{n} \cdot \nabla I(x) = \vec{n} \cdot \nabla \phi(x) + \vec{n} \cdot \nabla E(x) \geq 1 - |\vec{n} \cdot \nabla E_{\text{in}}(x)| - |\vec{n} \cdot \nabla E_{\text{out}}(x)|.$$

From Lemma 16, $|\vec{n} \cdot \nabla E_{\text{in}}(x)| < 1158\epsilon^2$ and from Lemma 17, $|\vec{n} \cdot \nabla E_{\text{out}}(x)| < 496\epsilon^2$. Hence,

$$\vec{n} \cdot \nabla I(x) > 1 - 1158\epsilon^2 - 496\epsilon^2 = 1 - 1654\epsilon^2 > 0$$

for $\epsilon \leq 1/50$. □

Theorem 18 also proves that the gradient can never be zero inside the ϵ-neighborhood. From Theorem 7, the zero set of I is inside the ϵ-neighborhood of F. Hence from the implicit function theorem [Bloomenthal 1997], zero is a regular value of I and the zero set U is a compact, two-dimensional manifold.

For a point $u \in U$, the normal of the reconstructed surface at u is given by $\vec{n}_u = \frac{\nabla I(u)}{\|\nabla I(u)\|}$. In the following theorem, we prove an upper bound on the angle between $\vec{n}_u$ and the normal of the point closest to u in F.

THEOREM 19. *Let u be a point on the reconstructed surface U whose closest point on F is p. Let $\vec{n}_u$ be the normal of U at point u, and let $\vec{n}$ be the normal of F at point p. An upper bound on the angle θ between $\vec{n}_u$ and $\vec{n}$ is given by,*

$$\cos\theta > \frac{1 - 1654\epsilon^2}{1 + 632\epsilon}.$$

PROOF. The angle between $\vec{n}_u$ and $\vec{n}$ is given by

$$\cos\theta = \frac{\vec{n} \cdot \nabla I(u)}{\|\nabla I(u)\|}.$$

From Theorem 18,

$$\vec{n} \cdot \nabla I(u) \geq 1 - 1654\epsilon^2.$$

Consider the following upper bound for $\|\nabla I(x)\|$,

$$\|\nabla I(u)\| \leq \|\nabla \phi(u)\| + \|\nabla E(u)\| \leq 1 + \|\nabla E_{\text{in}}(x)\| + \|\nabla E_{\text{out}}(u)\|.$$

From Lemma 16, $\|\nabla E_{\text{in}}(x)\| < 486\epsilon$ and from Lemma 17, $\|\nabla E_{\text{out}}(x)\| < 146\epsilon$. Hence,

$$\cos\theta > \frac{1 - 1654\epsilon^2}{1 + 632\epsilon}.$$ □

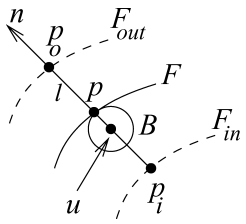

FIG. 8. Points p_i, p_o are the closest points to p on the offset surfaces. The line segment $p_i p_o$ intersects the zero set U at a unique point u.

6. *Topological Properties*

We now use the geometric results in Section 5 to show that the reconstructed surface U has the same topology as the sampled surface F. Our first topological result is that U is homeomorphic to F. As F and U are compact, a continuous, one-to-one, onto function from U to F defines a *homeomorphism*.

Definition 1. Let $\Gamma : \mathbb{R}^3 \to F$ map each point $q \in \mathbb{R}^3$ to the closest point of F.

THEOREM 20. *The restriction of* Γ *to* U *is a homeomorphism from* U *to* F.

PROOF. The discontinuities of Γ are the points on the medial axis of F. As U is constrained to be inside the ϵ-neighborhood of F, the restriction of Γ to U is continuous.

To show that Γ is onto, consider a point $p \in F$, and let $\vec{n}$ be the normal at p, as shown in Figure 8. Consider the line segment l parallel to $\vec{n}$ that intersects F_{out} and F_{in} at p_o and p_i, respectively. At each point $y \in p_o p_i$, $\nabla I(y) \cdot \vec{n} > 0$ from Theorem 18. So the function $I(x)$ is monotonically decreasing from p_o to p_i, and there is a unique point u on $p_o p_i$ where $I(u) = 0$. Let B be the ball of radius pu, centered at u as shown in Figure 8. As u is inside the ϵ-neighborhood of F, the ball B is strictly contained in one of the two medial balls touching p. Therefore the intersection of B and F is a single point p. From the definition of the function Γ, $\Gamma(u) = p$.

Finally we show that Γ is one-to-one. Assume there is another point $v \in U$ for which $\Gamma(v) = p$. Since $p_o p_i$ intersects U at a single point u, the point v has to be outside the segment $p_o p_i$. The distance from v to its closest point on F is greater than ϵ. This contradicts Theorem 14. □

Amenta et al. [2003] propose ambient isotopy as the condition for topological equivalence in computer graphics. We now show that U is *isotopic* to F which intuitively means that U can be continuously deformed into F without any change in topology.

Definition 2. An isotopy between two compact orientable surfaces in $\mathbb{R}^3$ is a continuous map $\Psi : U \times [0, 1] \to \mathbb{R}^3$, such that $\Psi(., 0)$ is the identity of U, $\Psi(., 1) = F$, and for each $t \in [0, 1]$, $\Psi(., t)$ is homeomorphic to U.

Definition 3. An ambient isotopy between two compact orientable surfaces U and F is a continuous map $\Psi : \mathbb{R}^3 \times [0, 1] \to \mathbb{R}^3$, such that $\Psi(., 0)$ is the identity of $\mathbb{R}^3$, $\Psi(U, 1) = F$, and for each $t \in [0, 1]$, $\Psi(., t)$ is a homeomorphism of $\mathbb{R}^3$.

THEOREM 21. *The zero surface U is isotopic to the sampled surface F.*

PROOF. We will define an ambient isotopy Ψ whose restriction to U will be an isotopy to F. Outside the ϵ-neighborhood, the ambient isotopy is the identity $\Psi(x, t) = x$ for $t \in [0, 1]$. From the proof of Theorem 20, we know that a line segment l normal to a point $p \in F$ intersects U only at one point u inside the ϵ-neighborhood. Let p_i and p_o be the endpoints of l on the inside and outside ϵ-offset surfaces, respectively, as shown in Figure 8. We define the ambient isotopy to be $\Psi(u, t) = tp + (1 - t)u$. The line segment $p_i u$ is linearly mapped to $p_i \Psi(u, t)$. Similarly, the line segment up_o is mapped to $\Psi(u, t)p_o$. □

The function $\Psi(., 1)$ given in the isotopy proof is a continuous function between two homeomorphic surfaces U, F, such that for each $u \in U$, we have $d(u, \Psi(u, 1)) \leq \epsilon$. This shows that the Fréchet distance [Fréchet 1924] between the sampled and the reconstructed surface is at most ϵ.

7. *Discussion*

Recall that the width of the Gaussian functions used in our algorithm depends on the smallest local feature size. As a result, our sampling requirements and the noise that can be handled are determined by the smallest local feature size of a point on F. Ideally, we would like to handle sampling proportional to the local feature size. When the width of the Gaussian weight functions is fixed, spacing between sample points in areas of the surface with large local feature size might be much larger than the width of the Gaussians. As a result, the reconstructed surface will be noisy and might have the wrong topology. One solution is to make the width of the Gaussian weight functions proportional to the spacing between sample points.

One disadvantage of our algorithm is that it requires sample normals. However, approximate sample normals can be easily obtained for laser range data by triangulating the range images. Each sample normal can be oriented using the location of the range scanner. When oriented normals are unavailable, the absolute distance to the tangent plane at each sample can be used instead of the signed distance as a point function to define a new function $I_u(x)$. The zero set of this function is hard to analyze as its gradient is not smooth near the sample points. However, the results in this article can be easily extended to show that the ϵ-level set of $I_u(x)$ consists of two components on each side of the surface, each homeomorphic to F.

The zero set of the cut function I only passes near the sample points, but we can construct a surface that interpolates the sample points with weight functions, such as $W_s(x) = \frac{e^{-\|x-s\|^2}}{\|x-s\|^2}$, that are infinite at the sample points. We can prove that the zero set is restricted to the ϵ-neighborhood when this weight function is used, but we could not prove results about the gradient approximations.

Our analysis of the MLS algorithm works in any dimension. The Lipschitz condition of Amenta and Bern [1999] in Theorem 1 and our results, which show that samples outside $B_2(x)$ have little effect on the cut function at point x, can be easily extended to higher dimensions. However, the value of ϵ required for the theoretical guarantees would decrease with increasing dimensionality.

It would be interesting to prove similar results for different weight functions and point functions. Gaussian weight functions that have infinite support yield a cut function defined everywhere. Our results show that we only pay a small penalty for

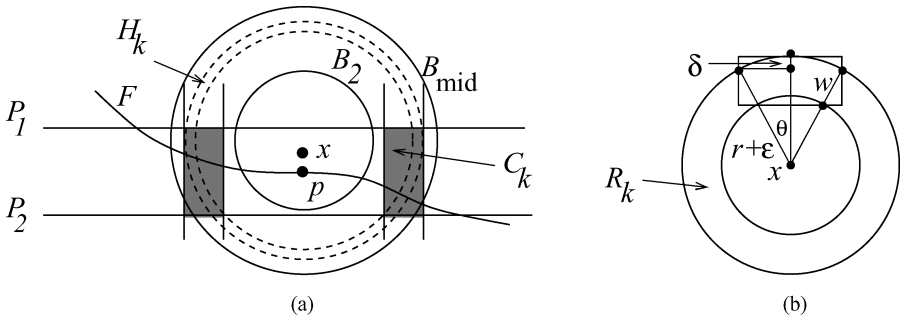

FIG. 9. (a) Point x is inside the ϵ-neighborhood, and p is the point closest to x on F. H_k is a spherical shell of width ϵ contained inside B_{mid}. The samples inside H_k are between two planes, P_1 and P_2 parallel to the tangent plane at p. A cylindrical annulus C_k whose cross section is the shaded region covers the region inside H_k between planes P_1, P_2. (b) The base of C_k is a ring R_k whose width is w. The ring R_k is divided into sectors such that the arc length of the outside circle within each sector is less than $\epsilon/\sqrt{3}$. Each sector is bounded by rectangle of length $l \leq \epsilon/\sqrt{3}$, and height $h \leq \delta + w$.

the infinite support, as the cut function at point x is mostly determined by samples inside $B_2(x)$. It might be easier to analyze other commonly used weight functions such as cubic B-splines that have compact support. Linear point functions are a poor representation of the sampled surface near sharp features. Distance functions of piecewise smooth surfaces might be used to better model such sharp features.

Appendix

PROOF OF LEMMA 11. We will cover the space inside H_k containing sample points with spheres of radius $\epsilon/2$ and use the upper bound on the weights of samples inside each ball of radius $\epsilon/2$ from Lemma 3 to get the desired result.

Let p be the point closest to x on the surface. As x is inside the ϵ-neighborhood, each sample $s \in H_k$ is inside a ball B of radius $r_k + 2\epsilon \leq r_{\text{mid}} + 2\epsilon < 1/4$, centered at p. Hence from Lemma 2, all samples inside B are squeezed between two parallel planes, P_1 and P_2, that are at a distance $(r_k + 2\epsilon + \epsilon^2)^2 + 2\epsilon^2$ apart, as shown in Figure 9.

The portion of space inside H_k that lies between the planes P_1, P_2 is contained inside a cylindrical annulus C_k whose cross section is the shaded region shown in Figure 9. The radius of the outer circle of C_k is $r + \epsilon$. To compute the inner radius, note that the distance from x to P_1, P_2 is at most $q = (r_k+2\epsilon+\epsilon^2)^2/2+\epsilon^2+\epsilon$. Hence, the radius of the smaller circle enclosing C_k is $r_i = \sqrt{r_k^2 - q^2}$. Let $w = r_k - r_i$ be the width of the annulus.

Let R_k be the base of the cylindrical annulus C_k. We begin by covering R_k with axis parallel squares of size $\epsilon/\sqrt{3}$. Divide the ring R_k into sectors such that the length of the outer arc inside each sector is $\epsilon/\sqrt{3}$. Each sector is contained in a rectangle, as shown in Figure 9(b). Clearly, the length of the rectangle is $l \leq \epsilon/\sqrt{3}$. The height of the rectangle is $h \leq \delta + w \leq \frac{\epsilon^2}{24(r+\epsilon)} + w$. So each sector can be covered with

$$t_1 = \frac{\sqrt{3}}{\epsilon} \times (h + \epsilon/\sqrt{3}) \leq \frac{\sqrt{3}}{\epsilon}\left(\frac{\epsilon^2}{24(r+\epsilon)} + w + \epsilon/\sqrt{3}\right)$$

squares of size $\epsilon/\sqrt{3}$. We add $\epsilon/\sqrt{3}$ to the height as squares in the covering which might extend out of the rectangle. The base R_k is divided into sectors of length $\epsilon/\sqrt{3}$ which means that the ring R_k can be covered with

$$t_2 = t_1 \times \left(\lceil \frac{2\sqrt{3}\pi}{\epsilon}(r_k + \epsilon) \rceil \right) \leq t_1 \times \left(\frac{2\sqrt{3}\pi}{\epsilon}(r_k + \epsilon) + 1 \right)$$

squares. We can now fill the cylindrical annulus C_k by stacking cubes of size $\epsilon/\sqrt{3}$ on top of these squares. The number of cubes required to cover C_k is

$$t_1 \times t_2 \times \frac{\sqrt{3}}{\epsilon}((r_k + 2\epsilon + \epsilon^2)^2 + 2\epsilon^2 + \epsilon/\sqrt{3}).$$

Each cube in this grid is covered by a sphere of radius $\epsilon/2$. Applying Lemma 3 to each sphere and simplifying using the inequality $\epsilon \leq r_0/\sqrt{12} \leq r_k/\sqrt{12}$, we can show that

$$\sum_{s_i \in H_2} \frac{1}{a_i} < 6\frac{r_k^3}{\epsilon^3}.$$

PROOF OF LEMMA 17. Recall that x is a point inside the ϵ-neighborhood and p is the point closest to x on F. The contribution of samples outside $B_2(x)$ to $\nabla E(x)$ is given by

$$\begin{aligned} \nabla E_{\text{out}}(x) \;=\; & \sum_{s_i \notin B_2(x)} \frac{(\vec{n} - \vec{n}_i)W_i(x)}{W(x)} \\ & + \sum_{s_i \notin B_2(x) \vee s_j \notin B_2(x)} \frac{2W_i(x)W_j(x)\delta_i(x)(s_i - s_j)}{\epsilon^2 W^2(x)}. \end{aligned} \tag{16}$$

Here, $\vec{n}$ is the surface normal at p. The first term in Equation (16) can be written as a summation over samples inside spherical shell H_k outside $B_2(x)$,

$$\frac{1}{W(x)} \sum_{k=0}^{k=\infty} \sum_{s_i \in H_k} (\vec{n} - \vec{n}_i)W_i(x).$$

Consider the second term T in Equation (16). Assume without loss of generality that the indices of samples are in the increasing order of distance to x. We can write the term T as

$$T = \sum_{s_i \notin B_2(x), i > j} \frac{2W_i(x)W_j(x)(\delta_i(x) - \delta_j(x))(s_i - s_j)}{\epsilon^2 W^2(x)}. \tag{17}$$

For each spherical shell H_k we define a set S_k containing pairs of samples,

$$S_k = \{(s_i, s_j) \,|\, i > j, s_i \in H_k\}.$$

Intuitively, s_i is inside the shell H_k, and s_j is inside the larger sphere that surrounds H_k. The summation in Equation (17) can now be written as

$$T = \frac{2}{\epsilon^2 W^2(x)} \sum_{k=0}^{k=\infty} \sum_{(s_i, s_j) \in S_k} W_i(x)W_j(x)(\delta_i(x) - \delta_j(x))(s_i - s_j). \tag{18}$$

Consider the norm of T,

$$\begin{aligned}\|T\| &\leq \frac{2}{\epsilon^2 W^2(x)} \sum_{k=0}^{k=\infty} \sum_{(s_i,s_j)\in S_k} W_i(x) W_j(x) |\delta_i(x) - \delta_j(x)| \|(s_i - s_j)\| \\ &< \frac{2}{\epsilon^2 W(x)} \sum_{k=0}^{k=\infty} \sum_{s_i \in S_k} W_i(x) \max\{|\delta_i(x) - \delta_j(x)| \|(s_i - s_j)\| \ |(s_i, s_j) \in S_k\}.\end{aligned}$$

So the expression for $\|\nabla E_{\text{out}}(x)\|$ can be written as

$$\begin{aligned}\|\nabla E_{\text{out}}(x)\| \leq \frac{1}{W(x)} \sum_{k=0}^{k=\infty} \sum_{s_i \in H_k} W_i(x) (\|\vec{n} - \vec{n}_i\| \\ + \frac{2}{\epsilon^2} \max\{|\delta_i(x) - \delta_j(x)| \|s_i - s_j\| \ |(s_i, s_j) \in S_k\}). \qquad (19)\end{aligned}$$

We split the summation in this equation into $\|\nabla E_1(x)\|$, containing the contributions of all shells $H_k \in B_{\text{mid}}(x)$, and $\|\nabla E_2(x)\|$, containing shells $H_k \notin B_{\text{mid}}(x)$.

As x is inside the ϵ-neighborhood, for each sample s_i inside shell H_k, $d(p, s_i) \leq r + 2\epsilon$. From Equation (8), for each sample s_i that is inside $H_k \in B_{\text{mid}}(x)$, $\|n - n_i\| \leq \Theta(r_k + 2\epsilon) < 4r_k$, and from Equation (9), $|\delta_i(x) - \delta_j(x)| \leq |\delta_i(x)| + |\delta_j(x)| \approx 12.5 r_k^2$. Since s_i, s_j are inside a ball of radius $r_k + 2\epsilon$ at p,

$$|\delta_i(x) - \delta_j(x)| \times \|s_i - s_j\| \leq 12.5 r_k^2 \times 2(r_k + 2\epsilon) < 40 r_k^3.$$

Substituting this upper bound into Equation (19), $\|\nabla E_1(x)\|$ can be written as

$$\|\nabla E_1(x)\| < \frac{1}{W(x)} \sum_{k=0}^{r_k \leq r_{\text{mid}}} \sum_{s_i \in H_k} \left(4r_k + \frac{80 r_k^3}{\epsilon^2}\right) \frac{e^{-r_k^2/\epsilon^2}}{a_i}.$$

In Lemma 11, we derived a bound on the weights of samples in each shell $H_k \in B_{\text{mid}}(x)$.

$$\begin{aligned}\|\nabla E_1(x)\| &\leq \frac{6}{W(x)\epsilon^3} \sum_{k=0}^{r_k \leq r_{\text{mid}}} \left(4r_k + \frac{80 r_k^3}{\epsilon^2}\right) r_k^3 e^{-r_k^2/\epsilon^2} \\ &\leq \frac{9}{W(x)\epsilon^3} \left(4r_0 + \frac{80 r_0^3}{\epsilon^2}\right) r_0^3 e^{-r_0^2/\epsilon^2}.\end{aligned}$$

Substituting the lower bound for $W(x)$ from Equation (3),

$$\|\nabla E_1(x)\| \leq \frac{72}{\epsilon^3}\left(4r_0 + \frac{80 r_0^3}{\epsilon^2}\right) r_0^3 e^{-(r_0^2 - (|\phi(x)| + \epsilon^2)^2} = \frac{72}{\epsilon^3} \left(4r_0 + \frac{80 r_0^3}{\epsilon^2}\right) r_0^3 e^{-12}.$$

Now consider shells H_k when $r_k \geq r_{\text{mid}}$. In this case, $\|n - n_i\| \leq 2$ and, from Equation (4), we know that, $|\delta_i(x) - \delta_j(x)| \leq |\delta_i(x)| + |\delta_j(x)| \leq 4(r_k + \epsilon)$. Since, s_i, s_j are inside H_k,

$$|\delta_i(x) - \delta_j(x)| \times \|s_i - s_j\| \leq 4(r_k + \epsilon) \times 2(r_k + \epsilon) < 14 r_k^2.$$

From the upper bound on the weight of samples inside H_k from Lemma (4),

$$\|\nabla E_2(x)\| \leq \frac{300}{W(x)\epsilon^2} \sum_{r_k=r_{\text{mid}}}^{\infty} \left(2 + \frac{28r_k^2}{\epsilon^2}\right) r_k^2 e^{-r_k^2/\epsilon^2} \leq \frac{3600e^4}{\epsilon^2} \times \left(2 + \frac{28r_{\text{mid}}^2}{\epsilon^2}\right) r_{\text{mid}}^2 e^{-r_{\text{mid}}^2/\epsilon^2}.$$

Note that for x inside the ϵ-neighborhood, $r_0 \leq 4\epsilon$. An upper bound on $\|\nabla E_{\text{out}}(x)\|$ is given by,

$$\begin{aligned}\|\nabla E_{\text{out}}(x)\| &\leq \|\nabla E_1\| + \|\nabla E_2(x)\| \\ &\leq \frac{72}{\epsilon^3}\left(4r_0 + \frac{80r_0^3}{\epsilon^2}\right) r_0^3 e^{-12} + \frac{3600e^4}{\epsilon^2}\left(2 + \frac{28r_{\text{mid}}^2}{\epsilon^2}\right) r_{\text{mid}}^2 e^{-r_{\text{mid}}^2/\epsilon^2} \\ &< 146\epsilon.\end{aligned}$$

We will now get an upper bound on $|\vec{n} \cdot \nabla E_{\text{out}}(x)$. Consider a sample s_i inside shell $H_k \in B_{\text{mid}}(x)$. From Equation (8),

$$\vec{n} \cdot (\vec{n} - \vec{n}_i) = 1 - \cos\Theta(r_k + 2\epsilon) \leq \Theta^2(r_k + 2\epsilon)/2 < 5r^2,$$

and, from Lemma 2, we know that s_i is between two planes P_1 and P_2 orthogonal to $\vec{n}$ that are at a distance $(r_k + 2\epsilon + \epsilon^2)^2 + 2\epsilon^2$ apart. From Equation (9) ,

$$|(\delta_i(x) - \delta_j(x)) \times \vec{n} \cdot (s_i - s_j)| \leq 12.5r_k^2 \times ((r_k + 2\epsilon + \epsilon^2)^2 + 2\epsilon^2) < 34r_k^4.$$

It is now easy to show that,

$$|\vec{n} \cdot \nabla E_1(x)| \leq \frac{72}{\epsilon^3}\left(5r_0^2 + \frac{68r_0^4}{\epsilon^2}\right) r_0^3 e^{-12},$$

and,

$$|\vec{n} \cdot \nabla E_2(x)| \leq \frac{3600e^4}{\epsilon^2}\left(2 + \frac{28r_{\text{mid}}^2}{\epsilon^2}\right) r_{\text{mid}}^2 e^{-r_{\text{mid}}^2/\epsilon^2}.$$

Adding the two terms we get,

$$|\vec{n} \cdot \nabla E_{\text{out}}(x)| < \frac{72}{\epsilon^3}\left(5r_0^2 + \frac{68r_0^4}{\epsilon^2}\right) r_0^3 e^{-12} + \frac{3600e^4}{\epsilon^2} \times \left(2 + \frac{28r_{\text{mid}}^2}{\epsilon^2}\right) r_{\text{mid}}^2 e^{-r_{\text{mid}}^2/\epsilon^2} < 496\epsilon^2. \quad \square$$

ACKNOWLEDGMENT. I would like to thank Jonathan Shewchuk for conversations that inspired the proof of Lemma 6 and for helping me improve this article. I would also like to thank Nina Amenta and James O'Brien for helpful discussions on MLS methods and François Labelle for pointing out an error in an earlier version of the article.

REFERENCES

ADAMSON, A. AND ALEXA, M. 2003. Approximating and intersecting surfaces from points. In *Proceedings of the Eurographics Symposium on Geometry Processing*. Eurographics Association, 230–239.

ALEXA, M., BEHR, J., COHEN-OR, D., FLEISHMAN, S., LEVIN, D., AND T. SILVA, C. 2003. Computing and rendering point set surfaces. *IEEE Trans. Visualiz. Comput. Graph. 9,* 1, 3–15.

AMENTA, N. AND BERN, M. 1999. Surface reconstruction by voronoi filtering. *Discr. Comput. Geom. 22*, 481–504.

AMENTA, N., CHOI, S., DEY, T. K., AND LEEKHA, N. 2002. A simple algorithm for homeomorphic surface reconstruction. *Int. J. Comp. Geom. Appli 12,* 1–2, 125–141.

AMENTA, N., CHOI, S., AND KOLLURI, R. 2001. The power crust. In *Proceedings of the 6th Symposium on Solid Modeling*. ACM, 249–260.

AMENTA, N. AND KIL, Y. 2004. Defining point-set surfaces. In *Proceedings of ACM SIGGRAPH*. ACM.

AMENTA, N., PETERS, T. J., AND RUSSELL, A. C. 2003. Computational topology: Ambient isotopic approximation of 2-manifolds. *Theor. Comput. Scie. 305,* 1, 3–15.

BELYTSCHKO, T., KRONGAUZ, Y., FLEMING, M., ORGAN, D., AND LIU, W. K. 1996. Meshless methods: An overview and recent developments. *J. Computat. Appl. Math. 74*, 111–126.

BLOOMENTHAL, J., Ed. 1997. *Introduction to Implicit Surfaces*. Morgan Kaufman.

BOISSONNAT, J.-D. AND CAZALS, F. 2000. Smooth surface reconstruction via natural neighbour interpolation of distance functions. In *Proceedings of the 16th Annual Symposium on Computational Geometry*. ACM, 223–232.

BOISSONNAT, J.-D., COHEN-STEINER, D., AND VEGTER, G. 2004. Isotopic implicit surface meshing. In *Proceedings of the 36th Annual ACM Symposium on Theory of Computing*. 301–309.

BOISSONNAT, J. D. AND OUDOT, S. 2003. Provably good surface sampling and approximation. In *Proceedings of the Eurographics Symposium on Geometry Processing*. Eurographics Association, 9–18.

CARR, J. C., BEATSON, R. K., CHERRIE, J. B., MITCHELL, T. J., FRIGHT, W. R., MCCALLUM, B. C., AND EVANS, T. R. 2001. Reconstruction and Representation of 3D objects with radial basis functions. In *Computer Graphics SIGGRAPH Proceedings*. 67–76.

CURLESS, B. AND LEVOY, M. 1996. A Volumetric method for building complex models from range images. In *Computer Graphics SIGGRAPH' Proceedings*. 303–312.

DEY, T. K. AND GOSWAMI, S. 2004. Provable surface reconstruction from noisy samples. In *Proceedings of the 20th Annual ACM Symposium on Computational Geometry*.

DEY, T. K. AND SUN, J. 2005. An adaptive MLS surface for reconstruction with guarantees. In *Proceedings of the Eurographics Symposium on Geometry Processing*. 43–52.

FLEISHMAN, S., ALEXA, M., COHEN-OR, D., AND SILVA, C. T. 2003. Progressive point set surfaces. *ACM Trans. Comput. Grap. 22,* 4.

FRÉCHET, M. 1924. Sur La Distance de Deux Surfaces. *Ann. Soc. Polonaise Math. 3*, 4–19.

HOPPE, H., DEROSE, T., DUCHAMP, T., MCDONALD, J., AND STUETZLE, W. 1992. Surface reconstruction from unorganized points. In *Computer Graphics SIGGRAPH Proceedings*. 71–78.

LANCASTER, P. AND SALKAUSKAS, K. 1981. Surfaces generated by moving least squares methods. *Math. Comput. 37,* 155, 141–158.

LEVIN, D. 2003. Mesh-independent surface interpolation. In *Geometric Modeling for Scientific Visualization*, G. Brunett, B. Hamann, K. Mueller, and L. Linsen, Eds. Springer-Verlag.

LEVOY, M., PULLI, K., CURLESS, B., RUSINKIEWICZ, S., KOLLER, D., PEREIRA, L., GINZTON, M., ANDERSON, S., DAVIS, J., GINSBERG, J., SHADE, J., AND FULK, D. 2000. The Digital Michelangelo Project: 3D scanning of large statues. In *Computer Graphics SIGGRAPH Proceedings*. 131–144.

LORENSEN, W. E. AND CLINE, H. E. 1987. Marching cubes: A high resolution 3D surface construction algorithm. In *Computer Graphics (SIGGRAPH Proceedings)*. 163–170.

MITRA, N. J., GELFAND, N., POTTMANN, H., AND GUIBAS, L. 2004. Registration of point cloud data from a geometric optimization perspective. In *Symposium on Geometry Processing*.

MITRA, N. J., NGUYEN, A., AND GUIBAS, L. 2004. Estimating surface normals in noisy point cloud data. *Int. J. Comput. Geom. Appl. 14,* 4–5, 261–276.

OHTAKE, Y., BELYAEV, A., ALEXA, M., TURK, G., AND SEIDEL, H.-P. 2003. Multi-level partition of unity implicits. *ACM Trans. Graph. 22,* 3, 463–470.

OSHER, S. AND FEDKIW, R. 2003. *The Level Set Method and Dynamic Implicit Surfaces*. Springer-Verlag, Berlin, Germany.

PAULY, M., KEISER, R., KOBBELT, L. P., AND GROSS, M. 2003. Shape modeling with point-sampled geometry. *ACM Trans. Graph. 22,* 3, 641–650.

PLANTINGA, S. AND VEGTER, G. 2004. Isotopic approximation of implicit curves and surfaces. In *Proceedings of the Eurographics/ACM SIGGRAPH Symposium on Geometry Processing*. ACM, 245–254.

SETHIAN, J. A. 1999. *Level Set Methods and Fast Marching Methods*. Cambridge Monograph on Applied and Computational Mathematics. Cambridge University Press.

SHEN, C., O'BRIEN, J. F., AND SHEWCHUK, J. R. 2004. Interpolating and approximating implicit surfaces from polygon soup. In *Proceedings of ACM SIGGRAPH*.

SHEPARD, D. 1968. A two-dimensional interpolation function for irregularly-spaced data. In *Proceedings of the 23rd ACM National Conference*. ACM, 517–524.

TURK, G. AND O'BRIEN, J. 1999. Shape transformation using variational implicit functions. In *Computer Graphics SIGGRAPH Proceedings*. 335–342.

ZHAO, H.-K., OSHER, S., AND FEDKIW, R. 2001. Fast surface reconstruction using the level set method. In *1st IEEE Workshop on Variational and Level Set Methods*. 194–202.

RECEIVED MAY 2005; REVISED OCTOBER 2006; ACCEPTED APRIL 2007